Analysis of channel-dropping tunnelling processes in photonic crystals with multiple vertical multi-mode cavities

2000 J. Phys. A: Math. Gen. 33 7761

(http://iopscience.iop.org/0305-4470/33/43/307)

J. Phys. A: Math. Gen. **33** (2000) 7761–7771. Printed in the UK PII: S0305-4470(00)12807-0

Analysis of channel-dropping tunnelling processes in photonic crystals with multiple vertical multi-mode cavities

Jian Fu†, Sailing He†‡ and Sanshui Xiao†§

† Centre for Optical and Electromagnetic Research, State Key Laboratory for Modern Optical Instrumentation, Zhejiang University, Yu-Quan, Hangzhou 310027, People's Republic of China
‡ Department of Electromagnetic Theory, Royal Institute of Technology, S-100 44 Stockholm, Sweden
§ Department of Physics, Zhejiang University, Hangzhou 310027, People's Republic of China

Received 22 March 2000, in final form 17 July 2000

Abstract. A theoretical analysis is given for a channel-drop tunnelling structure composed of two horizontal channels and a resonator system with multiple vertical multi-mode cavities in a two- or three-dimensional photonic crystal. Criteria for a complete transfer are derived for the application of wavelength division multiplexing. Compared to the resonator system with multiple (horizontal) single-mode cavities, the present resonator system improves the transport properties due to its high-order characteristics of the tunnelling process.

1. Introduction

A photonic crystal is a periodic dielectric structure which is used to control and manipulate the propagation of light [1–4]. It may offer a possibility of eliminating electromagnetic wave propagation within a frequency band, i.e. a photonic bandgap. The discovery of photonic bandgap materials and their use in controlling light propagation is a new and exciting development. It has vast implications for material scientists, electrical engineers and physicists. It is well known that one can create a waveguide (i.e. channel) in an otherwise perfect photonic crystal by making a line defect (e.g. removing a row of inclusions) [2]. Recently, channel-dropping tunnelling processes have attracted particular interest due to their important applications in, e.g., wavelength division multiplexing (WDM) in optical communications [5–8]. A channel-dropping tunnelling process occurs between two channels of propagating states, side coupled through a resonator system which supports localized states. Optimal tunnelling is reached when a propagating state at a fixed (selected) frequency is completely transferred from one channel to the other, leaving all other states (at other frequencies) unaffected [9]. In contrast to ordinary waveguides and cavities, photonic crystal waveguides and microcavities do not suffer from intrinsic radiation losses [1, 10–13] and are somewhat insensitive to fabrication-related disorders [14]. It is therefore of great practical interest to explore the possibilities of optimal tunnelling in photonic crystals. In [9, 15], it has been shown that optimal tunnelling between channels through two *horizontal single-mode* cavities in a two-dimensional photonic crystal can occur by creating resonant states of different symmetry and forcing an accidental degeneracy of the *renormalized* resonant frequency. Theoretical analysis and computer simulation have also been given there for an optimal tunnelling of the structure with two *horizontal single-mode* cavities.

In this paper, we study two channels of propagating states, side coupled through a resonator system consisting of multiple *vertical multi-mode* cavities (such as hexapole cavities) in a photonic crystal. We introduce a new formalism to obtain the transport properties of the channel-dropping tunnelling structure and derive criteria for the optimal tunnelling. It is shown that the present resonator system of the multiple vertical multi-mode cavities can improve the transport properties (compared with that of multiple horizontal single-mode cavities) and reach desirable higher-order channel-dropping tunnelling characteristics [6].

2. Problem formulation and the analysis

Figure 1(*a*) gives a schematic diagram of the higher-order channel-dropping tunnelling system considered in this paper. The physical configuration for such a structure in a photonic crystal is shown in figure 1(*b*). The system is composed of two channel states, labelled $|k\rangle$ (in the upper channel) and $|\bar{k}\rangle$ (in the lower channel), coupled through a resonator system. The resonator system consists of multiple vertical coupled multi-mode cavities which are formed by increasing the radii of the rods (note that a multi-mode state can be excited only for a cavity rod with radius larger than the inclusion rods). The corresponding multi-mode states are denoted by $|C^n\rangle$. The transport properties of the system are determined by the interaction between these states.

In order to eliminate the reflected and transmitted signals, one has to use a structure with two mirror symmetries with respect to planes perpendicular and parallel to the two channels [7]. The structure can be characterized by even and odd states with respect to the perpendicular mirror plane. The corresponding propagating states are labelled $|k_e\rangle$, $|\bar{k}_e\rangle$, $|k_o\rangle$, $|\bar{k}_o\rangle$, and the corresponding resonant states are labelled $|C_e^n\rangle$ and $|C_o^n\rangle$ (the even and odd states have subscripts e and o, respectively). We describe the interaction between these states by an effective Hamiltonian H which can be written as the sum of the even part and odd part, i.e. $H = H^e + H^o$, where

$$\begin{aligned} H^e = {} & \sum_{k>0} \omega(k_e)|k_e\rangle\langle k_e| + \sum_{\bar{k}>0} \omega(\bar{k}_e)|\bar{k}_e\rangle\langle \bar{k}_e| + \sum_{n=1}^{N} \omega_e^{(n)}|C_e^n\rangle\langle C_e^n| \\ & + \sum_{n=1}^{N-1} V_e^{(n,n+1)}[|C_e^n\rangle\langle C_e^{n+1}| + |C_e^{n+1}\rangle\langle C_e^n|] + \sqrt{\frac{2}{L}} \sum_{k>0} V_{k_e}[|k_e\rangle\langle C_e^1| + |C_e^1\rangle\langle k_e|] \\ & + \sqrt{\frac{2}{L}} \sum_{\bar{k}>0} V_{\bar{k}_e}[|\bar{k}_e\rangle\langle C_e^N| + |C_e^N\rangle\langle \bar{k}_e|] \end{aligned} \tag{1}$$

$$\begin{aligned} H^o = {} & \sum_{k>0} \omega(k_o)|k_o\rangle\langle k_o| + \sum_{\bar{k}>0} \omega(\bar{k}_o)|\bar{k}_o\rangle\langle \bar{k}_o| + \sum_{n=1}^{N} \omega_o^{(n)}|C_o^n\rangle\langle C_o^n| \\ & - \sum_{n=1}^{N-1} V_o^{(n,n+1)}[|C_o^n\rangle\langle C_o^{n+1}| + |C_o^{n+1}\rangle\langle C_o^n|] + \mathrm{i}\sqrt{\frac{2}{L}} \sum_{k>0} V_{k_o}[|k_o\rangle\langle C_o^1| - |C_o^1\rangle\langle k_o|] \\ & + \mathrm{i}\sqrt{\frac{2}{L}} \sum_{\bar{k}>0} V_{\bar{k}_o}[|\bar{k}_o\rangle\langle C_o^N| - |C_o^N\rangle\langle \bar{k}_o|] \end{aligned} \tag{2}$$

and where the frequencies $\omega(k_e)$, $\omega(\bar{k}_e)$, $\omega(k_o)$, $\omega(\bar{k}_o)$ give the dispersion relations of the even

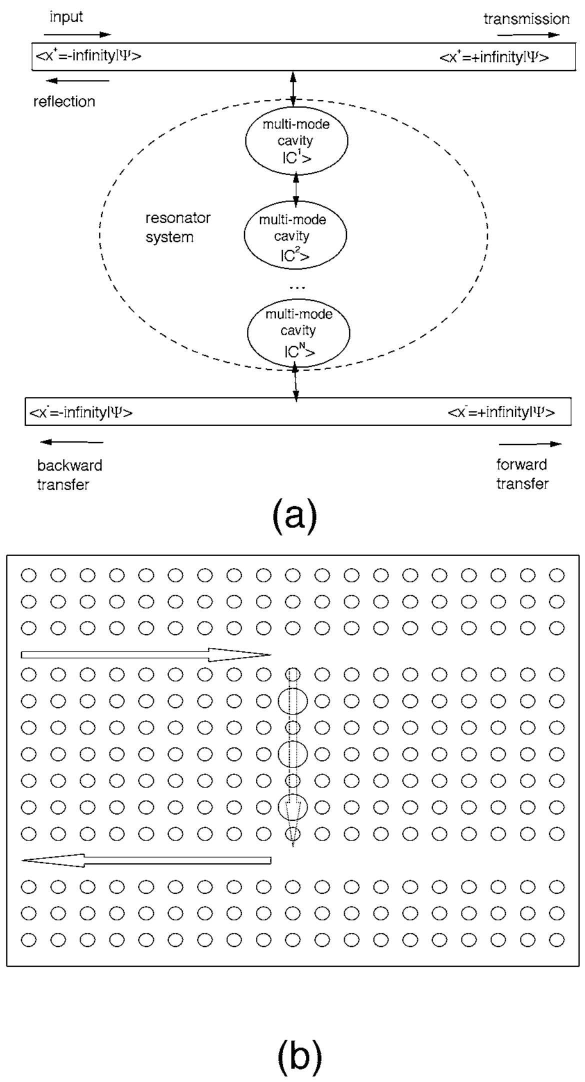

Figure 1. (*a*) A schematic diagram and (*b*) the configuration for a channel-drop tunnelling structure with a resonator system consisting of multiple vertical multi-mode cavities in a photonic crystal.

and odd states in the two channels, and

$$|k_e\rangle = \frac{1}{\sqrt{2}}(|k\rangle + |-k\rangle) \qquad |k_o\rangle = \frac{1}{\sqrt{2}\mathrm{i}}(|k\rangle - |-k\rangle)$$
$$|\bar{k}_e\rangle = \frac{1}{\sqrt{2}}(|\bar{k}\rangle + |-\bar{k}\rangle) \qquad |\bar{k}_o\rangle = \frac{1}{\sqrt{2}\mathrm{i}}(|\bar{k}\rangle - |-\bar{k}\rangle). \tag{3}$$

The factor $\frac{1}{\sqrt{L}}$ in equations (1), (2) arises from a box normalization of the length L. The coefficients V_{k_e}, $V_{\bar{k}_e}$, $V_{k\mathrm{o}}$, $V_{\bar{k}_o}$ are the coupling constants between the cavities and the propagating states, and the coefficient $V_e^{(n,n+1)}$ (or $V_o^{(n,n+1)}$) is the direct coupling constant between the localized states $|C_e^n\rangle$ and $|C_e^{n+1}\rangle$ (or $|C_o^n\rangle$ and $|C_o^{n+1}\rangle$). Due to the symmetry of the structure, the coupling coefficients satisfy the following relations:

$$
\begin{aligned}
&\omega(k_{\rm e}) = \omega(\bar{k}_{\rm e}) = \omega(k_{\rm o}) = \omega(\bar{k}_{\rm o}) \equiv \omega(k^{\rm in}) \\
&\omega_{\rm e}^{(1)} = \omega_{\rm e}^{(2)} = \cdots = \omega_{\rm e}^{(N)} \equiv \omega_{\rm e} \\
&\omega_{\rm o}^{(1)} = \omega_{\rm o}^{(2)} = \cdots = \omega_{\rm o}^{(N)} \equiv \omega_{\rm o} \\
&V_{\rm e}^{(1,2)} = V_{\rm e}^{(N-1,N)} \qquad V_{\rm e}^{(2,3)} = V_{\rm e}^{(N-2,N-1)} \qquad \cdots \\
&V_{\rm o}^{(1,2)} = V_{\rm o}^{(N-1,N)} \qquad V_{\rm o}^{(2,3)} = V_{\rm o}^{(N-2,N-1)} \qquad \cdots \\
&V_{k_{\rm e}} = V_{\bar{k}_{\rm e}} \equiv V_{k_{\rm e}} \\
&V_{k_{\rm o}} = V_{\bar{k}_{\rm o}} \equiv V_{k_{\rm o}}
\end{aligned}
\tag{4}
$$

where $k^{\rm in}$ is the wavevector for the incident wave.

Let us introduce a time-dependent state vector $|\Psi(t)\rangle$ to describe the whole structure (including the channels and cavities). The state vector can be decomposed into the even and odd parts, i.e.

$$|\Psi(t)\rangle = |\Psi^{\rm e}(t)\rangle + |\Psi^{\rm o}(t)\rangle. \tag{5}$$

Both $|\Psi^{\rm e}(t)\rangle$ and $|\Psi^{\rm o}(t)\rangle$ satisfy the following Schrödinger-type equation:

$$
\begin{aligned}
&{\rm i}\frac{\rm d}{{\rm d}t}|\Psi^{\rm e}(t)\rangle = H^{\rm e}|\Psi^{\rm e}(t)\rangle \\
&{\rm i}\frac{\rm d}{{\rm d}t}|\Psi^{\rm o}(t)\rangle = H^{\rm o}|\Psi^{\rm o}(t)\rangle.
\end{aligned}
\tag{6}
$$

Note that quantum mechanic theories such as the Schrödinger equation and Hamiltonian are commonly used in the literature of photonic crystals for theoretical analysis and the theoretical results have been shown to be consistent with the numerical simulation results obtained by solving the classical Maxwell's equations (see, e.g., [7, 9, 15, 16]). In this paper we use the Schrödinger equation (instead of Maxwell's equations) for the theoretical analysis.

We proceed by expanding $|\Psi^{\rm e}(t)\rangle$ and $|\Psi^{\rm o}(t)\rangle$ in terms of $|C_{\rm e}^n\rangle$, $|C_{\rm o}^n\rangle$, $|\bar{C}_{\rm e}^n\rangle$, $|\bar{C}_{\rm o}^n\rangle$ and $|k_{\rm e}\rangle$, $|k_{\rm o}\rangle$, $|\bar{k}_{\rm e}\rangle$, $|\bar{k}_{\rm o}\rangle$ as follows:

$$
\begin{aligned}
|\Psi(t)\rangle = &\sum_{n=1}^{N} C_{\rm e}^{(n)}(t)|C_{\rm e}^n\rangle + \sum_{n=1}^{N} C_{\rm o}^{(n)}(t)|C_{\rm o}^n\rangle + \sum_{k>0} C_{\rm e}(k,t)|k_{\rm e}\rangle + \sum_{k>0} C_{\rm o}(k,t)|k_{\rm o}\rangle \\
&+ \sum_{\bar{k}>0} C_{\rm e}(\bar{k},t)|\bar{k}_{\rm e}\rangle + \sum_{\bar{k}>0} C_{\rm o}(\bar{k},t)|\bar{k}_{\rm o}\rangle
\end{aligned}
$$

where the time-dependent amplitudes $C_{\rm e}^{(n)}(t)$, $C_{\rm o}^{(n)}(t)$, $C_{\rm e}(k,t)$, $C_{\rm o}(k,t)$, $C_{\rm e}(\bar{k},t)$ and $C_{\rm o}(\bar{k},t)$ are given by

$$
\begin{aligned}
&C_{\rm e}^{(n)}(t) = \langle C_{\rm e}^n|\Psi^{\rm e}(t)\rangle \qquad C_{\rm o}^{(n)}(t) = \langle C_{\rm o}^n|\Psi^{\rm o}(t)\rangle \\
&C_{\rm e}(k,t) = \langle k_{\rm e}|\Psi^{\rm e}(t)\rangle \qquad C_{\rm o}(k,t) = \langle k_{\rm o}|\Psi^{\rm o}(t)\rangle \\
&C_{\rm e}(\bar{k},t) = \langle \bar{k}_{\rm e}|\Psi^{\rm e}(t)\rangle \qquad C_{\rm o}(\bar{k},t) = \langle \bar{k}_{\rm o}|\Psi^{\rm o}(t)\rangle.
\end{aligned}
\tag{7}
$$

First we study the transport properties for the even part. The time-dependent amplitudes $C_{\rm e}^{(n)}(t)$, $C_{\rm e}(k,t)$ and $C_{\rm e}(\bar{k},t)$ satisfy the following Schrödinger equations:

$$
\begin{aligned}
&{\rm i}\frac{{\rm d}C_{\rm e}^{(1)}(t)}{{\rm d}t} = \omega_{\rm e}C_{\rm e}^{(1)}(t) + V_{\rm e}^{(1,2)}C_{\rm e}^{(2)}(t) + \sqrt{\frac{2}{L}}\sum_{k>0} V_{k_{\rm e}}C_{\rm e}(k,t) \\
&{\rm i}\frac{{\rm d}C_{\rm e}^{(n)}(t)}{{\rm d}t} = \omega_{\rm e}C_{\rm e}^{(n)}(t) + V_{\rm e}^{(n,n+1)}C_{\rm e}^{(n+1)}(t) + V_{\rm e}^{(n,n-1)}C_{\rm e}^{(n-1)}(t) \qquad n = 2, 3, \ldots, N-1 \\
&{\rm i}\frac{{\rm d}C_{\rm e}^{(N)}(t)}{{\rm d}t} = \omega_{\rm e}C_{\rm e}^{(N)}(t) + V_{\rm e}^{(N-1,N)}C_{\rm e}^{(N-1)}(t) + \sqrt{\frac{2}{L}}\sum_{\bar{k}>0} V_{k_{\rm e}}C_{\rm e}(\bar{k},t)
\end{aligned}
\tag{8}
$$

$$\begin{aligned} \mathrm{i}\frac{\mathrm{d}C_\mathrm{e}(k,t)}{\mathrm{d}t} &= \omega(k)C_\mathrm{e}(k,t) + \sqrt{\frac{2}{L}}V_{k_\mathrm{e}}C_\mathrm{e}^{(1)}(t) \\ \mathrm{i}\frac{\mathrm{d}C_\mathrm{e}(\bar{k},t)}{\mathrm{d}t} &= \omega(k)C_\mathrm{e}(\bar{k},t) + \sqrt{\frac{2}{L}}V_{k_\mathrm{e}}C_\mathrm{e}^{(N)}(t). \end{aligned} \tag{9}$$

Integrating equation (9) with the initial condition $|\Psi(t=0)\rangle = |k^{\mathrm{in}}\rangle$, one obtains the following time-dependent amplitudes, with $C_\mathrm{e}(k,t)$ and $C_\mathrm{e}(\bar{k},t)$ in terms of $C_\mathrm{e}^{(1)}(t)$ and $C_\mathrm{e}^{(N)}(t)$:

$$\begin{aligned} C_\mathrm{e}(k,t) &= \left[\mathrm{e}^{-\mathrm{i}\omega(k)t} + \sqrt{\frac{2}{L}}\int_0^\infty \mathrm{e}^{-\mathrm{i}\omega(k)(t-t')}V_{k_\mathrm{e}}C_\mathrm{e}^{(1)}(t')\,\mathrm{d}t'\right]\delta(k-k^{\mathrm{in}}) \\ C_\mathrm{e}(\bar{k},t) &= \left[\sqrt{\frac{2}{L}}\int_0^\infty \mathrm{e}^{-\mathrm{i}\omega(k)(t-t')}V_{k_\mathrm{e}}C_\mathrm{e}^{(N)}(t')\,\mathrm{d}t'\right]\delta(k-k^{\mathrm{in}}). \end{aligned} \tag{10}$$

Substituting the above equations into equation (8), one obtains

$$\begin{aligned} \mathrm{i}\frac{\mathrm{d}C_\mathrm{e}^{(1)}(t)}{\mathrm{d}t} &= \omega_\mathrm{e}C_\mathrm{e}^{(1)}(t) + V_\mathrm{e}^{(1,2)}C_\mathrm{e}^{(2)}(t) + \sqrt{\frac{2}{L}}V_{k_\mathrm{e}}\mathrm{e}^{-\mathrm{i}\omega(k^{\mathrm{in}})t} + \int_0^\infty G_\mathrm{e}(t-t')C_\mathrm{e}^{(1)}(t')\,\mathrm{d}t' \\ \mathrm{i}\frac{\mathrm{d}C_\mathrm{e}^{(n)}(t)}{\mathrm{d}t} &= \omega_\mathrm{e}C_\mathrm{e}^{(2)}(t) + V_\mathrm{e}^{(n,n+1)}C_\mathrm{e}^{(n+1)}(t) + V_\mathrm{e}^{(n,n-1)}C_\mathrm{e}^{(n-1)}(t) \qquad n=2,3,\ldots,N-1 \\ \mathrm{i}\frac{\mathrm{d}C_\mathrm{e}^{(N)}(t)}{\mathrm{d}t} &= \omega_\mathrm{e}C_\mathrm{e}^{(N)}(t) + V_\mathrm{e}^{(N-1,N)}C_\mathrm{e}^{(N-1)}(t) + \int_0^\infty G_\mathrm{e}(t-t')C_\mathrm{e}^{(N)}(t')\,\mathrm{d}t' \end{aligned} \tag{11}$$

where the delayed Green function $G_\mathrm{e}(t-t')$ is given by

$$G_\mathrm{e}(t-t') = \lim_{\varepsilon\to 0^+}\begin{cases} 0 & \text{if} \quad t<t' \\ \dfrac{2}{L}\displaystyle\int_0^\infty V_{k_\mathrm{e}}^2\mathrm{e}^{-\mathrm{i}[\omega(k)-\mathrm{i}\varepsilon](t-t')}\delta(k-k^{\mathrm{in}})\,\mathrm{d}k & \text{if} \quad t>t' \end{cases} \tag{12}$$

and its implicit form strongly depends on the dispersion relations. For example, in the photonic crystal waveguides, the Green function $G_\mathrm{e}(t-t')$ has the form of delta-function $\delta(t-t')$ as in a free space, rather than $G_\mathrm{e}(t-t') \sim (t-t')^{-1/2}$ at the edge of the isotropic PBG. Therefore, the variable t' in $C_\mathrm{e}^{(1)}(t')$ and $C_\mathrm{e}^{(N)}(t')$ in equation (11) can be replaced by t and $C_\mathrm{e}^{(1)}(t)$, $C_\mathrm{e}^{(N)}(t)$ can then be taken out of the integral [17]. The integral of $G_\mathrm{e}(t-t')$ can be calculated easily as for the free space case (see, e.g., [18]) and equations (11) can be written in the following form:

$$\begin{aligned} \mathrm{i}\frac{\mathrm{d}C_\mathrm{e}^{(1)}(t)}{\mathrm{d}t} &= \omega_\mathrm{e}C_\mathrm{e}^{(1)}(t) + V_\mathrm{e}^{(1,2)}C_\mathrm{e}^{(2)}(t) + \sqrt{\frac{2}{L}}V_{k_\mathrm{e}}\mathrm{e}^{-\mathrm{i}\omega(k^{\mathrm{in}})t} - \mathrm{i}V_{k_\mathrm{e}}^2 g_0^{-1}C_\mathrm{e}^{(1)}(t) \\ \mathrm{i}\frac{\mathrm{d}C_\mathrm{e}^{(n)}(t)}{\mathrm{d}t} &= \omega_\mathrm{e}C_\mathrm{e}^{(n)}(t) + V_\mathrm{e}^{(n,n+1)}C_\mathrm{e}^{(n+1)}(t) + V_\mathrm{e}^{(n,n-1)}C_\mathrm{e}^{(n-1)}(t) \qquad n=2,3,\ldots,N-1 \\ \mathrm{i}\frac{\mathrm{d}C_\mathrm{e}^{(N)}(t)}{\mathrm{d}t} &= \omega_\mathrm{e}C_\mathrm{e}^{(N)}(t) + V_\mathrm{e}^{(N-1,N)}C_\mathrm{e}^{(N-1)}(t) - \mathrm{i}V_{k_\mathrm{e}}^2 g_0^{-1}C_\mathrm{e}^{(N)}(t) \end{aligned} \tag{13}$$

where g_0 is the density of states of the propagating mode at frequency ω_e, i.e.

$$g_0^{-1} = \frac{2\pi}{L}\sum_{k^{\mathrm{in}}}\delta[\omega(k^{\mathrm{in}})-\omega_\mathrm{e}].$$

Note that the densities of states are equal to the inverse of the group velocity at that frequency ω_e (see, e.g., [9]).

Using equation (13) and the fact that $C_{\rm e}^{(n)}(t) = C_{\rm e}^{(n)}{\rm e}^{-{\rm i}\omega(k^{\rm in})t}$ (this is because the system is excited by a monochromatic wave with time-dependency ${\rm e}^{-{\rm i}\omega(k^{\rm in})t}$), it follows from equation (11) that

$$\begin{aligned}
\omega(k^{\rm in})C_{\rm e}^{(1)}{\rm e}^{-{\rm i}\omega(k^{\rm in})t} &= \omega_{\rm e}C_{\rm e}^{(1)}{\rm e}^{-{\rm i}\omega(k^{\rm in})t} + V_{\rm e}^{(1,2)}C_{\rm e}^{(2)}{\rm e}^{-{\rm i}\omega(k^{\rm in})t}\\
&\quad+\sqrt{\frac{2}{L}}V_{k_{\rm e}}{\rm e}^{-{\rm i}\omega(k^{\rm in})t} - {\rm i}\frac{|V_{k_{\rm e}}|^2}{g_0}C_{\rm e}^{(1)}{\rm e}^{-{\rm i}\omega(k^{\rm in})t} \qquad n = 2, 3, \ldots, N-1\\
\omega(k^{\rm in})C_{\rm e}^{(n)}{\rm e}^{-{\rm i}\omega(k^{\rm in})t} &= \omega_{\rm e}C_{\rm e}^{(n)}{\rm e}^{-{\rm i}\omega(k^{\rm in})t} + V_{\rm e}^{(n,n+1)}{\rm e}^{-{\rm i}\omega(k^{\rm in})t} + V_{\rm e}^{(n,n-1)}C_{\rm e}^{(n-1)}{\rm e}^{-{\rm i}\omega(k^{\rm in})t}\\
\omega(k^{\rm in})C_{\rm e}^{(N)}{\rm e}^{-{\rm i}\omega(k^{\rm in})t} &= \omega_{\rm e}C_{\rm e}^{(N)}{\rm e}^{-{\rm i}\omega(k^{\rm in})t} + V_{\rm e}^{(N-1,N)}C_{\rm e}^{(N-1)}{\rm e}^{-{\rm i}\omega(k^{\rm in})t} - {\rm i}\frac{|V_{k_{\rm e}}|^2}{g_0}C_{\rm e}^{(N)}{\rm e}^{-{\rm i}\omega(k^{\rm in})t}.
\end{aligned} \tag{14}$$

From the above system of linear equations, one can obtain the following explicit expressions for $C_{\rm e}^{(1)}$ and $C_{\rm e}^{(N)}$:

$$\begin{aligned}
C_{\rm e}^{(1)} &= \frac{\sqrt{\frac{2}{L}}V_{k_{\rm e}}}{\Delta\omega_{\rm e} + {\rm i}\gamma_{\rm e} - \frac{|V_{\rm e}^{(1,2)}|^2}{\Delta\omega_{\rm e} - \frac{|V_{\rm e}^{(2,3)}|^2}{\Delta\omega_{\rm e} - \cdots - \frac{|V_{\rm e}^{(N-1,N)}|^2}{\Delta\omega_{\rm e} + {\rm i}\gamma_{\rm e}}}}}\\
C_{\rm e}^{(N)} &= \frac{C_{\rm e}^{(1)}\prod_{n=1}^{N-1}V_{\rm e}^{(n,n+1)}}{[\Delta\omega_{\rm e} + {\rm i}\gamma_{\rm e}]\left[\Delta\omega_{\rm e} - \frac{|V_{\rm e}^{(N-1,N)}|^2}{\Delta\omega_{\rm e} + {\rm i}\gamma_{\rm e}}\right] \times \cdots \times \left[\Delta\omega_{\rm e} - \frac{|V_{\rm e}^{(2,3)}|^2}{\Delta\omega_{\rm e} - \frac{|V_{\rm e}^{(3,4)}|^2}{\Delta\omega_{\rm e} - \cdots - \frac{|V_{\rm e}^{(N-1,N)}|^2}{\Delta\omega_{\rm e} + {\rm i}\gamma_{\rm e}}}}\right]}
\end{aligned} \tag{15}$$

where

$$\Delta\omega_{\rm e} = \omega(k^{\rm in}) - \omega_{\rm e} \qquad \gamma_{\rm e} = \frac{V_{k_{\rm e}}^2}{g_0}. \tag{16}$$

Similarly, one can obtain the following time-dependent amplitudes $C_{\rm o}(k, t)$ and $C_{\rm o}(\bar{k}, t)$ for the odd part:

$$\begin{aligned}
C_{\rm o}(k, t) &= \left[{\rm e}^{-{\rm i}\omega(k)t} + {\rm i}\sqrt{\frac{2}{L}}\int_0^t {\rm e}^{-{\rm i}\omega(k)(t-t')}V_{k_{\rm o}}C_{\rm o}^{(1)}(t')\,{\rm d}t'\right]\delta(k - k^{\rm in})\\
C_{\rm o}(\bar{k}, t) &= \left[{\rm i}\sqrt{\frac{2}{L}}\int_0^t {\rm e}^{-{\rm i}\omega(k)(t-t')}V_{k_{\rm o}}C_{\rm o}^{(N)}(t')\,{\rm d}t'\right]\delta(k - k^{\rm in})
\end{aligned} \tag{17}$$

where

$$\begin{aligned}
C_{\rm o}^{(1)} &= \frac{-{\rm i}\sqrt{\frac{2}{L}}V_{k_{\rm o}}}{\Delta\omega_{\rm o} + {\rm i}\gamma_{\rm o} - \frac{|V_{\rm o}^{(1,2)}|^2}{\Delta\omega_{\rm o} - \frac{|V_{\rm o}^{(2,3)}|^2}{\Delta\omega_{\rm o} - \cdots - \frac{|V_{\rm o}^{(N-1,N)}|^2}{\Delta\omega_{\rm o} + {\rm i}\gamma_{\rm o}}}}}\\
C_{\rm o}^{(N)} &= \frac{(-1)^{N-1}C_{\rm o}^{(1)}\prod_{n=1}^{N-1}V_{\rm o}^{(n,n+1)}}{[\Delta\omega_{\rm o} + {\rm i}\gamma_{\rm o}]\left[\Delta\omega_{\rm o} - \frac{|V_{\rm o}^{(N-1,N)}|^2}{\Delta\omega_{\rm o} + {\rm i}\gamma_{\rm o}}\right] \times \cdots \times \left[\Delta\omega_{\rm o} - \frac{|V_{\rm o}^{(2,3)}|^2}{\Delta\omega_{\rm o} - \frac{|V_{\rm o}^{(3,4)}|^2}{\Delta\omega_{\rm o} - \cdots - \frac{|V_{\rm o}^{(N-1,N)}|^2}{\Delta\omega_{\rm o} + {\rm i}\gamma_{\rm o}}}}\right]}
\end{aligned} \tag{18}$$

with

$$\gamma_o = \frac{V_{k_o}^2}{g_0}. \tag{19}$$

Now we calculate the transmission, reflection and transfer amplitudes by evaluating the amplitudes of the state vector $\Psi(t)$ at x, $\bar{x} = \pm\infty$, which has the following asymptotic behaviour. The transmitted amplitude in the upper channel is given by

$$\begin{aligned}
\langle x = +\infty|\Psi(t)\rangle &= \sum_{k'>0}\langle x = +\infty|k'\rangle\langle k'|\Psi(t)\rangle \\
&= \tfrac{1}{2}\sum_{k'>0}[\langle x = +\infty|k_e'\rangle\langle k_e'|\Psi(t)\rangle - \mathrm{i}\langle x = +\infty|k_e'\rangle\langle k_o'|\Psi(t)\rangle] \\
&\quad +\tfrac{1}{2}\sum_{k'>0}[\langle x = +\infty|k_o'\rangle\langle k_o'|\Psi(t)\rangle + \mathrm{i}\langle x = +\infty|k_o'\rangle\langle k_e'|\Psi(t)\rangle] \\
&= \tfrac{1}{2}\left[\sum_{k'>0}\langle x = +\infty|k_e'\rangle + \mathrm{i}\sum_{k'>0}\langle x = +\infty|k_o'\rangle\right]C_e(k,t)\langle k_e'|k_e^{\mathrm{in}}\rangle \\
&\quad -\frac{\mathrm{i}}{2}\left[\sum_{k'>0}\langle x = +\infty|k_e'\rangle + \mathrm{i}\sum_{k'>0}\langle x = +\infty|k_o'\rangle\right]C_o(k,t)\langle k_o'|k_o^{\mathrm{in}}\rangle.
\end{aligned} \tag{20}$$

Since

$$\begin{aligned}
&\langle k_e'|k_e^{\mathrm{in}}\rangle = \langle k_o'|k_o^{\mathrm{in}}\rangle = \delta(k' - k^{\mathrm{in}}) \\
&C_e(k,t) = \mathrm{e}^{-\mathrm{i}\omega(k^{\mathrm{in}})t} + \int_0^t \sqrt{\frac{L}{2}}\frac{G_e(t-t')}{V_{k_e}}C_e^{(1)}(t')\,\mathrm{d}t' \\
&C_o(k,t) = \mathrm{e}^{-\mathrm{i}\omega(k^{\mathrm{in}})t} + \int_0^t \sqrt{\frac{L}{2}}\frac{G_o(t-t')}{V_{k_o}}C_o^{(1)}(t')\,\mathrm{d}t' \\
&\langle x|k_e'\rangle = \frac{1}{\sqrt{L}}\cos(k'x) \quad \langle x|k_o'\rangle = \frac{1}{\sqrt{L}}\sin(k'x)
\end{aligned}$$

where the Green function $G_o(t-t')$ for the odd part is given by

$$G_o(t-t') = \lim_{\varepsilon\to 0^+}\begin{cases} 0 & \text{if } t < t' \\ \dfrac{2}{L}\displaystyle\int_0^\infty V_{k_o}^2\mathrm{e}^{-\mathrm{i}[\omega(k)-\mathrm{i}\varepsilon](t-t')}\delta(k-k^{\mathrm{in}})\,\mathrm{d}k & \text{if } t > t' \end{cases}$$

it follows from equation (20) that (cf (15) and (17))

$$\begin{aligned}
\langle x = +\infty|\Psi(t)\rangle &= \lim_{x\to+\infty}\frac{L}{2\pi}\left\{\frac{1}{2\sqrt{L}}\int_0^\infty \mathrm{e}^{\mathrm{i}k'x}\delta(k'-k^{\mathrm{in}})\right. \\
&\quad\times\left[\mathrm{e}^{-\mathrm{i}\omega(k')t} + \int_0^t\sqrt{\frac{L}{2}}\frac{G_e(t-t')}{V_{k_e}}C_e^{(1)}(t')\,\mathrm{d}t'\right]\mathrm{d}k' - \frac{\mathrm{i}}{2\sqrt{L}}\int_0^\infty \mathrm{e}^{\mathrm{i}k'x}\delta(k'-k^{\mathrm{in}}) \\
&\quad\left.\times\left[\mathrm{e}^{-\mathrm{i}\omega(k')t} + \mathrm{i}\int_0^t\sqrt{\frac{L}{2}}\frac{G_o(t-t')}{V_{k_o}}C_o^{(1)}(t')\,\mathrm{d}t'\right]\mathrm{d}k'\right\} \\
&= \frac{1}{\sqrt{L}}\mathrm{e}^{-\mathrm{i}\omega(k^{\mathrm{in}})t+\mathrm{i}k^{\mathrm{in}}x}\left[1 - \sqrt{\frac{L}{2}}\frac{\mathrm{i}V_{k_e}C_e^{(1)}}{g_0} + \sqrt{\frac{L}{2}}\frac{V_{k_o}C_o^{(1)}}{g_0}\right] \\
&= \frac{\mathrm{e}^{-\mathrm{i}\omega(k^{\mathrm{in}})t+\mathrm{i}k^{\mathrm{in}}x}}{\sqrt{L}}\left[1 - \sqrt{\frac{L}{2}}\frac{\mathrm{i}\gamma_e C_e^{(1)}}{V_{k_e}} + \sqrt{\frac{L}{2}}\frac{\gamma_o C_o^{(1)}}{V_{k_o}}\right].
\end{aligned} \tag{21}$$

Other scatting amplitudes can be obtained in a similar fashion. The reflected amplitude in the upper channel is given by

$$\langle x = -\infty|\Psi(t)\rangle = \sum_{k'>0}\langle x = +\infty| - k'\rangle\langle -k'|\Psi(t)\rangle$$
$$= \frac{e^{-i\omega(k^{in})t - ik^{in}x}}{\sqrt{L}}\left[-\sqrt{\frac{L}{2}}\frac{i\gamma_e C_e^{(1)}}{V_{k_e}} - \sqrt{\frac{L}{2}}\frac{\gamma_o C_o^{(1)}}{V_{k_o}}\right]. \qquad (22)$$

The forward transfer amplitude in the lower channel is given by

$$\langle \bar{x} = +\infty|\Psi(t)\rangle = \sum_{\bar{k}'>0}\langle x = +\infty|\bar{k}'\rangle\langle \bar{k}'|\Psi(t)\rangle$$
$$= \frac{e^{-i\omega(\bar{k}^{in})t + i\bar{k}^{in}\bar{x}}}{\sqrt{L}}\left[-\sqrt{\frac{L}{2}}\frac{i\gamma_e C_e^{(N)}}{V_{k_e}} + \sqrt{\frac{L}{2}}\frac{\gamma_o C_o^{(N)}}{V_{k_o}}\right] \qquad (23)$$

where $|\bar{k}^{in}| = |k^{in}|$. The backward transfer amplitude in the lower channel is given by

$$\langle \bar{x} = -\infty|\Psi(t)\rangle = \sum_{\bar{k}'>0}\langle x = +\infty| - \bar{k}'\rangle\langle -\bar{k}'|\Psi(t)\rangle$$
$$= \frac{e^{-i\omega(\bar{k}^{in})t - i\bar{k}^{in}\bar{x}}}{\sqrt{L}}\left[-\sqrt{\frac{L}{2}}\frac{i\gamma_e C_e^{(N)}}{V_{k_e}} - \sqrt{\frac{L}{2}}\frac{\gamma_o C_o^{(N)}}{V_{k_o}}\right]. \qquad (24)$$

3. Transport properties of the higher-order channel-dropping tunnelling structure

One can obtain various filter functions through the appropriate selection of the direct coupling constant between the localized states $|C_e^n\rangle$ (or $|C_o^n\rangle$). In applications such as WDM in optical communications, such a maximum flat line shape is of great interest, due to its desired 'flat-top' and 'sharp-sidewall' characteristics [19]. Therefore, we focus on achieving the maximum flat filter functions. To eliminate the reflection in the upper channel, we choose $\Delta\omega_e = \Delta\omega_o \equiv \Delta\omega$, $\gamma_e = \gamma_o \equiv \gamma$, $V_e^{(n,n+1)} = V_o^{(n,n+1)} \equiv V^{(n,n+1)}$, i.e.,

$$\omega_e = \omega_o \qquad V_{k_e} = V_{k_o} \qquad V_e^{(n,n+1)} = V_o^{(n,n+1)}. \qquad (25)$$

Then one has

$$|\langle x = -\infty|\Psi(t)\rangle|^2 = 0 \qquad \text{for all} \quad \omega(k^{in}). \qquad (26)$$

Note that equation (25) is due to a so-called accidental degeneracy while equation (4) is due to the symmetry of the structure. By making use of condition (25), one can obtain the following spectra of the transmitted signal (for an incident signal of unit amplitude) in the upper channel:

$$|\langle x = +\infty|\Psi(t)\rangle|^2 = 1 - \frac{1}{P_N(|\Delta\omega|^2)} \qquad (27)$$

and the following spectra of the forward and backward transferred signals in the lower channel:

$$\left.\begin{aligned} T_+(\omega) &\equiv |\langle \bar{x} = +\infty|\Psi(t)\rangle|^2 = 0 \\ T_-(\omega) &\equiv |\langle \bar{x} = -\infty|\Psi(t)\rangle|^2 = \frac{1}{P_N(|\Delta\omega|^2)} \end{aligned}\right\} \quad \text{when} \quad N \text{ is odd} \qquad (28)$$

$$\left.\begin{aligned} T_+(\omega) &= \frac{1}{P_N(|\Delta\omega|^2)} \\ T_-(\omega) &= 0 \end{aligned}\right\} \quad \text{when} \quad N \text{ is even} \qquad (29)$$

where $P_N(|\Delta\omega|^2)$ is given by

$$P_N(|\Delta\omega|^2) = \frac{|\Delta\omega + \mathrm{i}\gamma|^2}{4|\gamma|^2 \prod_{n=1}^{N-1} |V^{(n,n+1)}|^2} \left| \Delta\omega - \frac{|V^{(N-1,N)}|^2}{\Delta\omega + \mathrm{i}\gamma} \right|^2 \times \cdots$$
$$\times \left| \Delta\omega - \cfrac{|V^{(2,3)}|^2}{\Delta\omega - \cfrac{|V^{(3,4)}|^2}{\Delta\omega - \cdots - \cfrac{|V^{(N-1,N)}|^2}{\Delta\omega + \mathrm{i}\gamma}}} \right|^2 \left| \Delta\omega + \mathrm{i}\gamma - \cfrac{|V^{(1,2)}|^2}{\Delta\omega - \cfrac{|V^{(2,3)}|^2}{\Delta\omega - \cdots - \cfrac{|V^{(N-1,N)}|^2}{\Delta\omega + \mathrm{i}\gamma}}} \right|^2 . \quad (30)$$

From equations (28) and (29), one sees that the transferred signal in the lower channel is backward when the number of the cavities is odd and is forward when the number of the cavities is even.

For a maximally flat response, the coefficients of all orders of $|\Delta\omega|^2$, except for the highest, must vanish [19]. This implies that for a resonator system consisting of N *vertical multi-mode* cavities, the inverse of the transferring coefficient in the lower channel is given by

$$P_N(|\Delta\omega|^2) = A_0 + A_N |\Delta\omega|^{2N} \quad (31)$$

where A_0, A_N are constants related to γ and $V^{(n,n+1)}$. To illustrate how the maximally flat response is achieved, we give a detailed analysis for a resonator system consisting of three *vertical multi-mode* cavities. By making use of the symmetry condition $V^{(1,2)} = V^{(2,3)} \equiv V$, the inverse of the transferring coefficient can be written in a polynomial form (cf equations (27), (28) and (30)):

$$P_N(|\Delta\omega|^2) = 4 + \frac{|\gamma|^4 - 4|\gamma|^2|V|^2 + 4|V|^4}{|\gamma|^2|V|^4}|\Delta\omega|^2 + 2\frac{|\gamma|^2 - 2|V|^2}{|\gamma|^2|V|^4}|\Delta\omega|^4 + \frac{1}{|\gamma|^2|V|^4}|\Delta\omega|^6. \quad (32)$$

A maximally flat response is achieved when $|\gamma|^2 = 2|V|^2$. Under this condition, the spectrum of the transferred signal in the lower channel is given by (cf equation (28))

$$T_-(\omega) = \frac{4\gamma^6}{|\Delta\omega|^6 + 4\gamma^6}. \quad (33)$$

Other cases can be considered in a similar fashion, and the results are summarized in table 1 for resonator systems consisting of 2–6 *vertical multi-mode* cavities.

In [7], the filter response of a resonator structure with two *horizontal single-mode* cavities was studied by an analytical method as well as a numerical finite-difference time-domain (FDTD) method. Excellent agreement for the spectra of the transmitted signal and transferred signal was obtained between the FDTD simulation and the analytical method when the coupling coefficients are chosen appropriately. In [15], a structure with a multi-mode single cavity was simulated by a numerical FDTD method. Using the same parameters ($\omega_0 = 0.341\,56$ $(2\pi c/a)$ and $\gamma = 0.3162 \times 10^{-4}$ $(2\pi c/a)$, where a is the period of the lattice), we calculate the spectra of the transmitted signal in the upper channel and transferred signal in the lower channel with the analytical formulae presented in this paper for a channel-drop tunnelling structure with multiple *vertical multi-mode* cavities. Figures 2(*a*) and (*b*) show the band characteristics of (*a*) the transferring coefficient and (*b*) the transmission coefficient, respectively, for a resonator structure with three vertical multi-mode cavities (solid curve), two vertical multi-mode cavities (dash–dotted curve) and a single multi-mode cavity (dashed curve). From figure 2 one sees clearly that the resonator structure with more vertical multi-mode cavities gives better transport

Table 1. Conditions for a maximally flat response of a resonant system consisting of multiple vertical multi-mode cavities. (N is the number of cavities.)

N	Conditions
2	$\|\gamma\|^2 = \|V\|^2$
3	$\|V^{(1,2)}\|^2 = \|V^{(2,3)}\|^2 = 0.5\|\gamma\|^2$
4	$\|V^{(1,2)}\|^2 = \|V^{(3,4)}\|^2 = 0.025\|\gamma\|^2$, $\|V^{(2,3)}\|^2 = 0.01\|\gamma\|^2$
5	$\|V^{(1,2)}\|^2 = \|V^{(4,5)}\|^2 = 0.023\,875\|\gamma\|^2$, $\|V^{(2,3)}\|^2 = \|V^{(3,4)}\|^2 = 0.007\,375\|\gamma\|^2$
6	$\|V^{(1,2)}\|^2 = \|V^{(5,6)}\|^2 = 0.022\,875\|\gamma\|^2$, $\|V^{(2,3)}\|^2 = \|V^{(4,5)}\|^2 = 0.006\,125\|\gamma\|^2$, $\|V^{(3,4)}\|^2 = 0.004\,475\|\gamma\|^2$

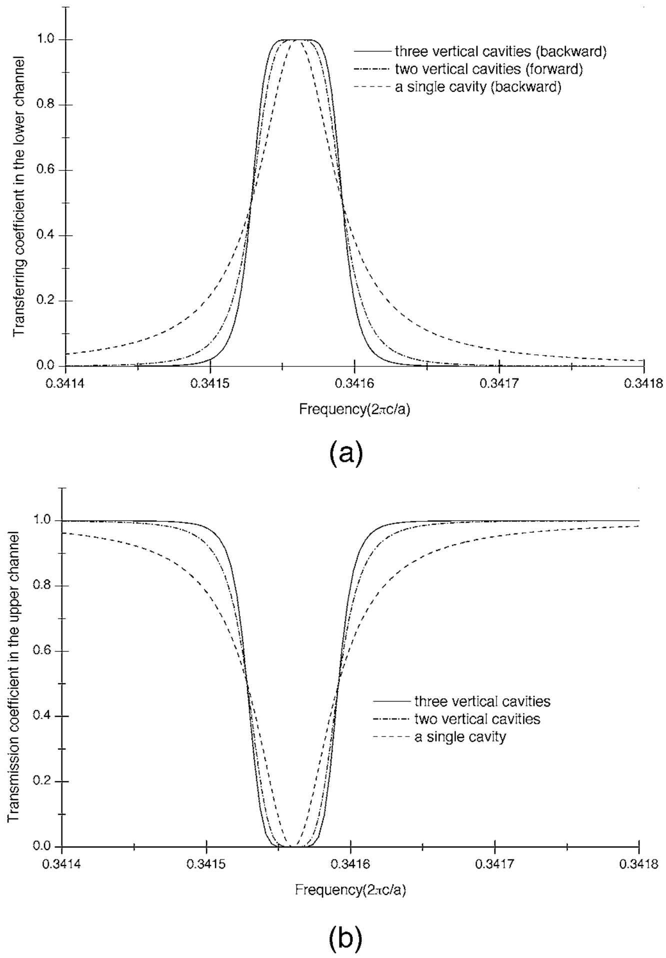

Figure 2. The band characteristics for a resonator system consisting of between one and three vertical multi-mode cavities. (*a*) The transferring coefficient in the lower channel. (*b*) The transmission coefficient in the upper channel.

properties, namely, a more narrow pass-band (or stop-band) and a flatter top, compared with the resonator structure with a single multi-mode cavity.

The quality factor (i.e., Q factor, which is defined as a ratio of the central frequency and the half-width of the pass-band) of a resonator is a measure of the frequency selectivity of the resonator. For the case of a resonator system with two *horizontal single-mode* cavities, the quality factor is about 1000 [7]. The present resonator system with multiple *vertical multi-mode* cavities gives a quality factor exceeding 5000.

4. Conclusion

In this paper we have given a theoretical analysis for a higher-order channel-drop tunnelling structure with a resonator system which consists of multiple *vertical multi-mode* cavities in photonic crystals. Criteria for a complete transfer have been derived for the application of WDM. Compared to a resonator system with two *single-mode* cavities or a *single multi-mode* cavity, the present resonator system (with multiple *vertical multi-mode* cavities) improves the transport properties and provides a narrower pass-band, a flatter top and a larger Q factor. The analysis and results hold for both two- and three-dimensional cases.

Acknowledgment

The partial support from a major grant of the Science & Technology Division of Zhejiang Province (China) is gratefully acknowledged.

References

[1] Yablonovitch E 1987 *Phys. Rev. Lett.* **58** 2059
[2] Joannopoulos J D, Mead R D and Winn J N 1995 *Photonic Crystals: Molding the Flow of Light* (Princeton, NJ: Princeton University Press)
[3] C M Soukoulis (ed) 1993 *Photonic Band Gaps and Localization: Proc. NATO ARW* (New York: Plenum)
[4] Joannopoulos J D, Villeneuve P R and Fan S 1997 *Nature* **386** 143
[5] Haus H A and Lai Y 1992 *J. Lightwave Technol.* **10** 57
[6] Little B E, Chu S T, Foresi J and Laine J-P 1997 *J. Lightwave Technol.* **15** 998
[7] Fan S, Villeneuve P R, Joannopoulos J D and Haus H A 1998 *Phys. Rev. Lett.* **80** 960
[8] He J J, Davies M and Koteles E S 1998 *J. Lightwave Technol.* **16** 631
[9] Fan S, Villeneuve P R, Joannopoulos J D, Khan M J, Manolatou C and Haus H A 1999 *Phys. Rev.* B **59** 15 882
[10] Villeneuve P R, Fan S and Joannopoulos J D 1996 *Phys. Rev.* B **54** 7837
[11] Qiu M and He S 1999 *Phys. Rev.* B **60** 10 610
[12] Qiu M and He S 2000 *Phys. Lett.* A **266** 425
[13] He S, Popov M, Qiu M and Simovski C R 2000 *Microwave Opt. Technol. Lett.* **25** 236
[14] Fan S, Villeneuve P R and Joannopoulos J D 1995 *J. Appl. Phys.* **78** 1415
[15] Fan S, Villeneuve P R, Joannopoulos J D and Haus H A 1998 *Opt. Express* **3** 4
[16] John S and Quang T 1991 *Phys. Rev.* B **43** 12 772
[17] John S and Quang T 1996 *Phys. Rev.* A **54** 4479
[18] Allen L and Eberly J H 1975 *Optical Resonance and Two-Level Atoms* (New York: Wiley) pp 163–4
[19] Little B E, Chu S T, Haus H A, Foresi J and Lain J-P 1997 *J. Lightwave Technol.* **15** 1149